Available online at www.sciencedirect.com
SCIENCE DIRECT®
Biochemical and Biophysical Research Communications 329 (2005) 362–369
BBRC
www.elsevier.com/locate/ybbrc

Charge effects modulate actin assembly by classic myelin basic protein isoforms ☆

Christopher M.D. Hill, George Harauz *

Department of Molecular and Cellular Biology, Biophysics Interdepartmental Group, University of Guelph, Guelph, Ont., Canada N1G 2W1

Received 20 January 2005

Abstract

Myelin basic protein (MBP), a highly cationic structural protein of the myelin sheath, is believed to be associated with the cytoskeleton in vivo and interacts with actin in vitro, but little is known about the regulation of this interaction. The rate and extent of actin polymerization induced by 18.5 kDa MBP charge isomers were correlated to charge reduction by post-translational modifications. Increased ionic strength attenuated the initial rate but not the final extent of polymerization achieved. Reduced pH enhanced the rate and extent of polymerization, presumably via partial protonation of intrinsic histidyl residues. The polymerizing activities of the 21.5, 17, and 14 kDa MBP splice variants were not proportionate to their net charges or charge densities. The presence of at least one region derived from exon II or VI of the "classic" MBP gene was required for effective bundling as assessed by light scattering and transmission electron microscopy.

Keywords: Myelin basic protein; Actin; Multiple sclerosis; Pyrene fluorescence; Transmission electron microscopy; Light scattering

Central nervous system myelin is formed by the extension of membranous cellular processes from oligodendrocytes [1]. Actin polymerization extends the leading edge of these processes, which are subsequently stabilized by microtubules [2], but it is unclear how this cytoskeletal remodelling is regulated [3]. Myelin basic protein (MBP), a highly cationic protein that maintains the lamellar compaction of the oligodendrocyte membrane within mature myelin, may also regulate the assembly of these cytoskeletal elements [4–8].

MBP exists as a family of developmentally regulated and post-translationally modified isoforms arising from alternate splicing of the Golli (genes of oligodendrocyte lineage) genetic unit, which includes the "classic" MBP gene [9,10]. The predominant 18.5 kDa MBP comprises a series of charge isomers denoted C1–C8, where C1 is least modified and most highly positively charged. C1 polymerizes globular actin (G-actin) in vitro under otherwise non-polymerizing conditions [5,6] and bundles filamentous actin (F-actin) [4]. Both activities are reversed by Ca^{2+}-calmodulin (CaM) which binds MBP [4,5]. In vivo, MBP isoforms containing a region derived from exon II of the classic MBP gene colocalize with actin and tubulin in the radial component, a series of tight junctions that span multiple myelin lamellae, and the expression of these isoforms is also increased during myelination [11]. *Shiverer* knockout mice which lack MBP exhibit substantial hypomyelination of central nervous system neurons and myelination of inappropriate targets [12], whereas oligodendrocytes cultured from these mice display extensive cytoskeletal disorganization and aberrant processes [13].

☆ *Abbreviations:* C1–C6, 18.5 kDa MBP charge isomers 1–6; CaM, calmodulin; CV, column volume; F-actin, filamentous actin; G-actin, globular actin; Golli, genes of oligodendrocyte lineage; MARCKS, myristoylated alanine-rich C kinase substrate; MBP, myelin basic protein; PTM, post-translational modification; rm, recombinant murine; TEM, transmission electron microscopy.

* Corresponding author. Fax: +1 519 837 2075.
E-mail address: gharauz@uoguelph.ca (G. Harauz).

0006-291X/$ - see front matter © 2005 Elsevier Inc. All rights reserved.
doi:10.1016/j.bbrc.2005.01.151

Many physiologically important actin binding proteins contain cationic regions which mediate their interaction with actin: calponin [14], MARCKS [15], and dystrophin [16]. MBP is highly flexible [10], which also suggests that its interaction with actin may be primarily determined by electrostatics. A previous study of the interaction of proteolytic fragments of 18.5 kDa rabbit MBP with actin concluded that MBP contained two terminal actin binding sites and that the degree of actin polymerization induced by each fragment was not related to its charge [6]. However, the fragment net charges quoted there were incorrect, and the recalculated values are indeed correlated to extent of polymerization induced (Supplementary Fig. 1). Several post-translational modifications (PTMs), including phosphorylation and deamidation, and deimination in developing myelin and in multiple sclerosis patients, result in a reduction of MBP cationicity [10,17]. Recently, amino acid replacements that mimic deimination (as in the C8 isoform) have been shown to alter the MBP–actin interaction, particularly MBP's actin-bundling activity and susceptibility to depolymerization induced by Ca^{2+}-CaM [8].

Both PTMs and alternate splicing of MBP may regulate its actin binding properties. Here, we demonstrate that the polymerization of actin by 18.5 kDa MBP is attenuated by a decrease in positive charge due to PTMs such as phosphorylation and deamidation in the C1–C6 charge isomers. The influence of ionic strength and pH on MBP-mediated actin polymerization is also shown to be consistent with an electrostatic mechanism. Additionally, we examine MBP isoforms known to be associated with actin in specialized structures within myelin, to determine the importance of regions derived from particular exons of the classic MBP gene.

Materials and methods

Proteins. Charge isomers of 18.5 kDa bovine MBP (C1 through C6 in order of decreasing net positive charge) were purified from the delipidated white matter of a 2-year-old steer brain [18]. Expression constructs containing cDNA for murine 18.5 kDa (rmC1, for recombinant murine C1), 14 kDa (rm14), 17 kDa (rm17), and 21.5 kDa (rm21) MBP isoforms, in addition to two terminal deletion mutants of the 18.5 kDa isoform (rmC1ΔC and rmC1ΔN), in pET22b(+) plasmid vectors (Novagen) were transformed into *Escherichia coli* BL21-CodonPlus(DE3)-RP (Stratagene). MBP variants were expressed and purified by nickel-chelation chromatography [19]. All MBP preparations were assessed by SDS–PAGE, and concentrations were determined with a BCA assay (Pierce Biotechnology, Rockford, IL) using a bovine C1 standard.

Actin purified from rabbit muscle was purchased from Cytoskeleton (Denver, CO) as was actin containing *N*-(1-pyrene) iodoacetamide covalently linked to Cys374. Lyophilized actin was resuspended in G-buffer (5 mM Tris–HCl, pH 8.0, 0.2 mM $CaCl_2$, 0.2 mM ATP, and 0.5 mM dithiothreitol), rapidly frozen in LN_2, and stored at −80 °C. Prior to use, actin was rapidly thawed, diluted with fresh G-buffer, incubated on ice for 1 h, and then centrifuged at 150,000*g* for 2 h at 4 °C to sediment oligomers. After centrifugation, the top 80% of the actin solution was carefully removed with a syringe and retained for polymerization assays. Calmodulin purified from bovine brain was purchased from Calbiochem (San Diego, CA).

Cation exchange chromatography. Fast protein liquid chromatography (FPLC) was used to quantify retention of recombinant MBP isoforms on a 1 mL sulfopropyl Sepharose column in an AKTA FPLC system (Amersham Biosciences, Piscataway, NJ). The column was equilibrated with five column volumes (CV) of buffer A (80 mM glycine, pH 10.0) containing 10% buffer B (80 mM glycine, pH 10.0, 1 M NaCl) by volume. To apply sample, a 200 μL loop containing 0.5 mg/mL MBP was voided using 1 mL (1 CV) of buffer A containing 10% buffer B. The column was washed by 4 CV of buffer A containing 10% buffer B, and a linear NaCl gradient from 10% to 40% buffer B was applied to elute MBP. Conductivity and A_{280} were monitored, and the elution conductivity for a given protein was chosen to correspond to the absorbance peak center. Elution conductivities were reproducible to within 0.5 mS/cm. All solutions were applied at 1 mL/min, buffers were filtered using 0.22 μm bottle top filters (Corning, Corning, NY), and all steps were performed at 4 °C.

Fluorescence assays. Actin polymerization was induced by MBP or salts and monitored by observing fluorescence enhancement of pyrenylated actin [20]. Pyrene-labelled actin was mixed with unlabelled actin to a final proportion of 5%. Sixty microliter samples of 5 μM actin solutions in G-buffer were loaded into a 3 mm × 3 mm quartz cuvette (Hellma Canada, Concord, ON), and fluorescence was recorded at 90°. An Alphascan-2 spectrofluorimeter (Photon Technology International, London, ON) was used to excite the sample at 365 nm with 1 nm bandwidth, and emission was measured at 407 nm with 4 nm bandwidth. Data were collected at the rate of 10/s and plotted relative to the sample fluorescence before polymerization. Fluorescence traces were smoothed using a negative exponential algorithm, and equilibrium values were determined using non-linear regression in Sigmaplot 7.101 (SPSS, Chicago, IL). Polymerization curves produced under the same conditions were highly reproducible within an experimental session.

For polymerization assays performed at pH 7.0, 600 mM imidazole–HCl, pH 7.0, was added simultaneously with the MBP or salts to a final concentration of 50 mM. A duplicate experiment using 600 mM imidazole–HCl, pH 8.0, was performed to test for effects due to imidazole alone.

Light scattering. Light scattering was measured at 90° with an Alphascan-2 spectrofluorimeter at an excitation wavelength of 365 nm with 4 nm bandwidth, and an emission wavelength of 375 nm with 4 nm bandwidth, following [14]. F-actin was prepared from G-actin in G-buffer by adding KCl and $MgCl_2$ to final concentrations of 50 and 2 mM, respectively (F-buffer), and incubating at room temperature for 1 h. For MBP titrations at different KCl concentrations, an MBP solution was added sequentially to 60 μL of a 2.5 μM F-actin solution in F-buffer with 30 or 100 mM KCl, in a 3 mm × 3 mm quartz cuvette, to MBP concentrations of 0.5, 1.0, 1.5, 2.0, and 2.5 μM. The sample was mixed by pipetting and allowed to equilibrate (2–5 min). The final scattering value was determined by averaging the count rate for 60 s, while collecting data at the rate of 10/s. Titrations were reproduced in triplicate and each point represents an average scattering value with an error of 1 SD.

A similar procedure was used to compare bundling induced by charge isomers or recombinant isoforms. Each MBP isoform/isomer was added to a solution of 2.5 μM F-actin in F-buffer to an equimolar final concentration. Scattering due to F-actin alone was subtracted from the scattering of each sample. Each sample was reproduced in triplicate and each point represents an average scattering value, corrected for dilution.

Transmission electron microscopy. Bundles of F-actin formed by MBP were prepared as for light scattering. 10 μL droplets of the bundle solution were applied to carbon-coated 400 mesh Cu grids and incubated for 2 min. Excess solution was wicked off with filter paper,

then 10 μL of 2% uranyl acetate was applied for 2 min, wicked off, and the grids were air-dried for transmission electron microscopy (TEM). Micrographs were recorded on a Leo912AB TEM (Leo GmbH, Oberkochen, Germany) operating at 100 kV with an EsiVision CCD-BM/1k SSCCD camera, at nominal magnifications of 20,000×–40,000×. Structures were considered to be representative when observed at four separate locations on triplicate grids. Fast Fourier transformation of images was performed using Scion Image Software (Scion, Frederick, MD).

Results and discussion

Effects of ionic strength and pH

The influence of ionic strength on polymerization of actin by MBP was tested using unmodified rmC1. The addition of rmC1 to G-actin in G-buffer with 30 mM KCl resulted in rapid polymerization with a negligible lag phase (Fig. 1), whereas increasing [KCl] resulted in longer lag times. The equilibrium fluorescence intensity of rmC1-mediated polymerization was similar at all [KCl] tested (4% variation) and control traces for polymerization induced by KCl alone are shown (Fig. 1). Although actin polymerization was faster in the presence of MBP at all [KCl] tested, the slower nucleation of actin polymerization at higher [KCl] is consistent with partial shielding of the electrostatic interaction between MBP and actin. For comparison, the intracellular $[K^+]+[Na^+]$ in oligodendrocytes is roughly 75–90 mM [21], but local changes in ionic strength may be effected as described in an intriguing alternate view of the myelin sheath as a perfusion pump [22].

The effect of ionic strength on the ability of rmC1 to bundle actin was assayed by titrating a fixed amount of F-actin with MBP while monitoring light scattering at 90°. The average scattering values observed at 30 and 100 mM KCl were similar in parallel titrations (Fig. 1B). F-actin bundles formed by equimolar amounts of rmC1 at these KCl concentrations (representing titration endpoints) were visualized by TEM. Bundles formed in 30 mM KCl were loosely packed, readily curved, and changed direction (Fig. 1C), whereas those formed at 100 mM KCl were thicker and straighter (Fig. 1D). It has been suggested that the ability of MBP to bundle F-actin arises from its ability to partially neutralize the filaments' charge [5], similar to calponin [14] and segments of MARCKS-related protein [15]. At higher ionic strength, further charge shielding of the MBP–actin filaments may allow them to come into even closer proximity, reinforcing the bundles.

A pH shift from 8 to 7 should increase protein cationicity by changing the histidyl residues from unprotonated to approximately 25% protonation. Here, the polymerizing activity of C1 was assayed at pH 8 and 7, with an expected average charge increase of +2.5 due to its 10 His. (C1 was used rather than rmC1, which

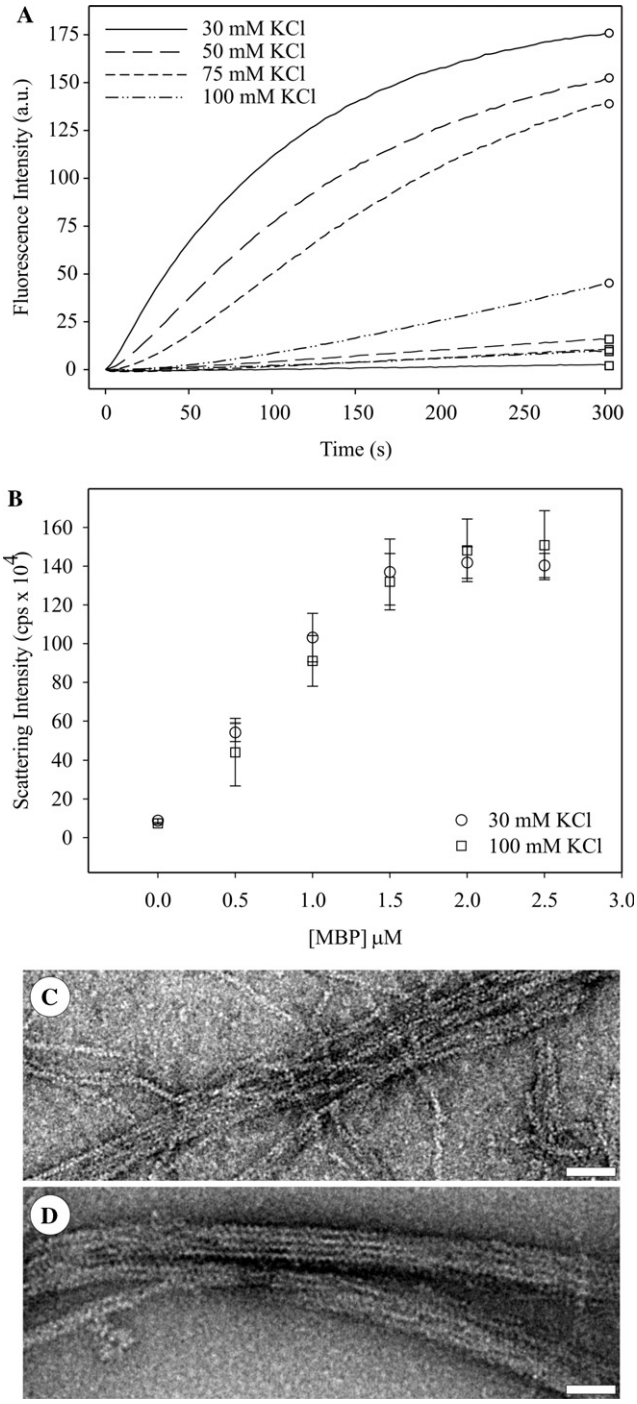

Fig. 1. (A) Effect of [KCl] on polymerization of G-actin by rmC1. rmC1 was mixed with 5 μM G-actin (5% pyrene labelled) in G-buffer at a 1:4 molar ratio with simultaneous addition of KCl to indicated final concentrations (traces terminated by circles). Parallel polymerizations effected by KCl alone are shown (traces terminated by squares). (B) Effect of [KCl] on bundling of F-actin by rmC1. rmC1 was sequentially added to 2.5 μM actin pre-polymerized by 50 mM KCl and 2 mM $MgCl_2$. Each point represents an average value for triplicate samples; error bars represent 1 SD. (C,D) Morphology of F-actin bundles formed by MBP at 30 mM KCl (C) and 100 mM KCl (D). An equimolar amount of rmC1 was added to 2.5 μM actin pre-polymerized by 50 mM KCl and 2 mM $MgCl_2$, and incubated for 1 h prior to staining by 2% uranyl acetate. Scale bars represent 50 nm.

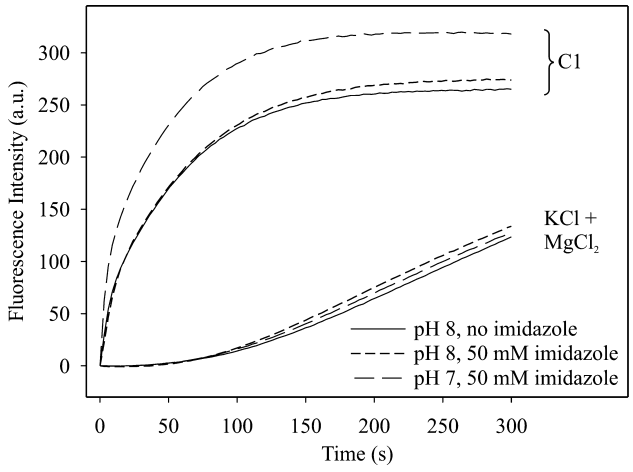

Fig. 2. Effect of pH on polymerizing activity of bovine 18.5 kDa MBP. Polymerization was effected by adding C1 to 5 μM G-actin (5% pyrene labelled) in G-buffer at a 1:4 molar ratio. 600 mM imidazole–HCl, pH 7 or 8, was added simultaneously to 50 mM in duplicate polymerizations. Polymerization effected by 50 mM KCl and 2 mM $MgCl_2$ alone is also shown.

had a hexahistidine tag.) Actin polymerization by C1 was greater at pH 7 in duplicate samples (Fig. 2). The reduction of the net negative charge of actin monomers due to a corresponding partial protonation of their His, which could reduce intermonomer repulsion and enhance polymerization, was minor, as seen by comparing polymerization induced by 50 mM KCl and 2 mM $MgCl_2$ at both pH values. The presence of imidazole, used to control pH, also had a negligible effect (Fig. 2). This result shows that an increase in net charge can enhance polymerization as readily as it can be inhibited by a decrease in net charge.

Effect of post-translational modifications

We used charge isomers C1-C6 of bovine 18.5 kDa MBP, with different degrees of modification (phosphorylation, deamidation, etc.) [23], to test the effect of charge reduction on MBP's ability to polymerize and bundle actin. Each isomer was mixed with actin at a molar ratio of 1:4 (MBP:actin), lower than the molar ratio of approximately 1:2 previously observed to result in maximal final fluorescence as determined by titration [5]. All charge isomers induced polymerization (Fig. 3A) in a standard pyrenyl-G-actin assay, and the initial rate of polymerization induced by each isomer was correlated to its net positive charge. The lag phase, associated with formation of nuclei, was observed in a control sample polymerized by 50 mM KCl and 2 mM $MgCl_2$ without MBP, but was not apparent when polymerization was induced by the charge isomers. The maximum intensity of the actin samples polymerized by the charge isomers was also correlated to their net charge. The maximum fluorescence intensity of the F-buffer control was measured 1 h after addition of KCl and $MgCl_2$, and was approximately 85% higher than the final intensity observed for C1 (not shown). There was a 20-fold difference in the initial rate, and a 2-fold difference in the final fluorescence intensity, for polymerization induced by C1 compared to C6, the most and least cationic isomers tested.

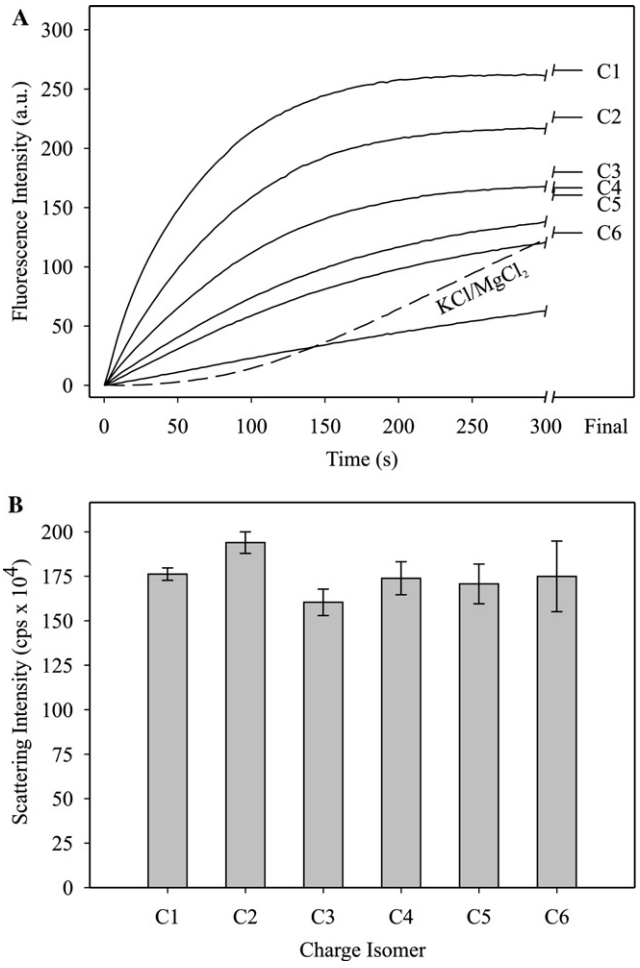

Fig. 3. (A) Polymerization of G-actin by charge isomers of natural bovine 18.5 kDa MBP (solid lines). Polymerization was effected by adding C1–C6 to 5 μM G-actin (5% pyrene labelled) in G-buffer at a 1:4 molar ratio. Polymerization effected by 50 mM KCl and 2 mM $MgCl_2$ alone is shown (dashed line). (B) Bundling of F-actin by charge isomers of bovine 18.5 kDa MBP. An equimolar amount of C1–C6 was added to 2.5 μM actin pre-polymerized by 50 mM KCl and 2 mM $MgCl_2$. Counts per second (cps) shown are relative to scattering of F-actin prior to addition of MBP. Values represent an average value for triplicate samples; error bars represent 1 SD.

Charge reduction of MBP by phosphorylation alters its interaction with phospholipid bilayers [24] and its secondary structure [25]. Here, the reduction in the extent of polymerization induced by reduced charge isomers indicates that PTMs may shift the binding equilibrium of MBP such that it binds to, and stabilizes into filaments, a smaller fraction of the available G-actin pool. Phosphorylation could serve as a reversible mech-

anism for modulating the propensity of MBP to polymerize actin in vivo and to bind membranes [26]. This result contrasts with the relatively minor reduction in polymerizing ability caused by pseudo-deimination [8], and suggests that the location of charge reduction in the sequence also influences polymerizing activity.

The ability of the charge isomers to bundle F-actin was assayed by combining an equimolar amount of F-actin and MBP, and measuring the resulting 90° light scattering. In contrast to the differences in polymerization ability, the six isomers bundled F-actin to a similar extent (Fig. 3B). The more extensively modified isomers may bind polymerized actin as readily as unmodified MBP, if the filaments do not require MBP to maintain their stability. Alternatively, different mechanisms may effect actin polymerization and bundling by MBP. If so, PTMs may reduce polymerizing ability by reducing MBP cationicity, whereas bundling could be effected by intermolecular interactions between MBP molecules bound to different F-actin filaments.

Effect of alternate splicing

Recombinant murine forms of the rarer 21.5, 17.22, and 14 kDa variants (denoted as rm21, rm17, and rm14) were used here in addition to rmC1 (18.5 kDa) (Fig. 4A) [9]. The terminal deletion mutants rmC1ΔC and rmC1ΔN were also used [27]. As the charge isomers of natural MBP are defined by the order in which they elute from a cation exchange column [18], these recombinant proteins were subjected to cation exchange FPLC under non-denaturing conditions to rank their charge characteristics. The conductivity values at which the MBP variants elute were proportionate to their linear charge density (λ, Table 1). The only divergences occurred for rmC1 and rmC1ΔC, as the C-terminal deletion mutant eluted earlier despite having the same charge density as the full-length variant, albeit with a lower net positive charge.

The polymerizing activities of the splice isoforms were assayed via pyrenyl-actin fluorescence (Fig. 4B). Neither the initial rates nor the final values of fluorescence were proportionate to either the net charge or charge density. The full-length isoforms were more effective at polymerizing actin than the deletion mutants. The reduced polymerizing abilities of rm21 and rm17 relative to rmC1 were unexpected, as both of these isoforms share a common region derived from exon II of the classic MBP gene, and are closely associated with regions of cytoskeletal enrichment in vivo. These MBP isoforms may have different structures that result in reduced binding efficiencies. The attenuated abilities of the rmC1 terminal deletion mutants to polymerize G-actin may have been due to the large reductions in their net charges or, in view of the results for the splice variants, to loss of structures required for binding. Even

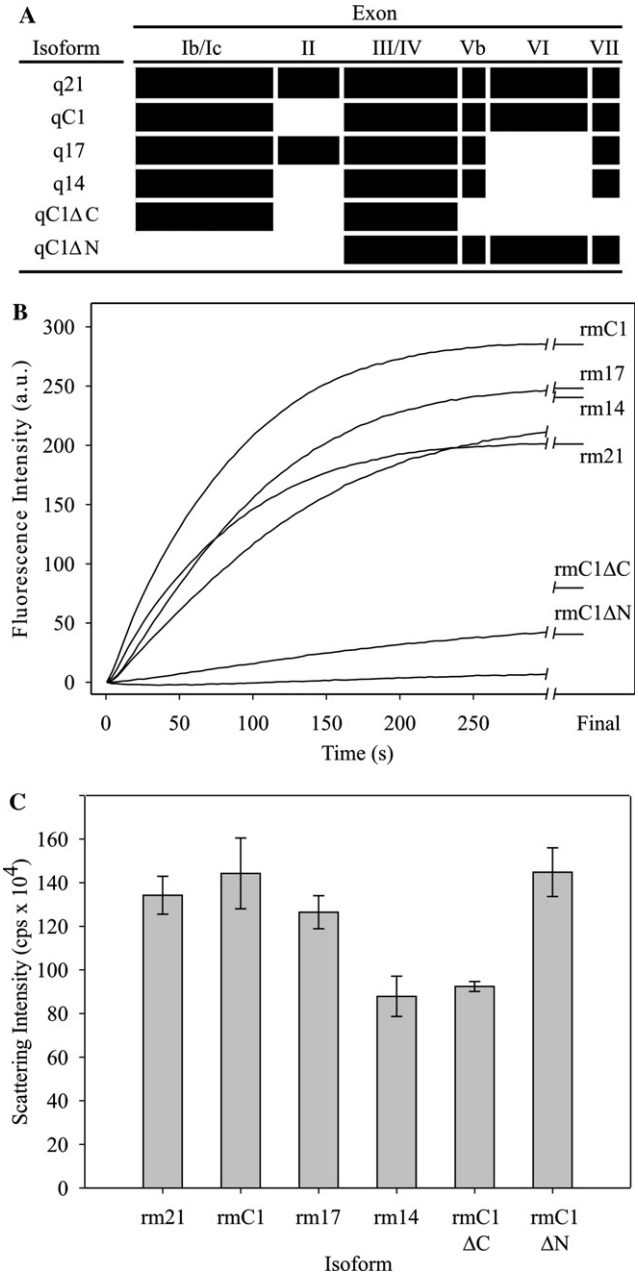

Fig. 4. Recombinant classic and deletion isoforms of murine MBP used here. (A) Schematic depiction of genetic origin of classic murine isoforms (Swiss-Prot primary Accession No. P04370). (B) Polymerization of G-actin by rmMBP isoforms. Polymerization was effected by adding an rmMBP isoform to 5 μM G-actin (5% pyrene labelled) in G-buffer at a 1:4 molar ratio. (C) Bundling of F-actin by rmMBP isoforms. An equimolar amount of each isoform was added to 2.5 μM actin pre-polymerized by 50 mM KCl and 2 mM $MgCl_2$. Counts per second (cps) shown are relative to scattering of F-actin prior to addition of MBP. Values represent an average value for triplicate samples; error bars represent 1 SD.

though the isoforms containing regions derived from exon II exhibited less actin polymerizing activity than rmC1, they still effected substantial polymerization (roughly 70% and 85% of the final intensity induced by rmC1, respectively). These results show that the exon

Table 1
Recombinant murine MBP isoforms

Isoform	Length (aa)	Molecular mass (Da)	Net charge	p*I*	λ (charge/aa)	FPLC elution (mS/cm)
rm21	202	22411.1	+23	11.01	0.144	27.6 ± 0.5
rmC1	176	19421.5	+19	11.00	0.108	24.7
rm17	160	18003.1	+19	11.59	0.119	29.3
rm14	135	15218.9	+15	11.64	0.111	27.3
rmC1ΔC	111	12453.7	+12	11.39	0.108	20.4
rmC1ΔN	121	13401.8	+11	10.47	0.091	17.3

Average linear charge density (λ) calculated as net charge (from numbers of Glu, Asp, Lys, and Arg) divided by length (including C-terminal hexahistidine tag and linker).

II isoforms could, indeed, have significant direct interactions with actin in the radial component of myelin. The 18.5 kDa and exon II isoforms are phosphorylated to similar extents in vivo [28], and their interactions with actin could also be regulated by reversible PTMs. Phosphorylation of the latter isoforms regulates their nuclear translocation during oligodendrocyte development [29].

The F-actin-bundling activity of the classic isoforms was assayed by 90° light scattering (Fig. 4C). The average scattering counts for rm21, rmC1, rm17, and rmC1ΔN were similar within experimental error. Both rm14 and rmC1ΔC increased the count rate to a similar extent, but scattering was reduced in comparison to other isoforms. TEM showed that whereas rm21 and rm17, like rmC1, were able to promote the formation of tight bundles, rm14 resulted in the formation of only very loose assemblies resembling bales of straw (Fig. 5). Paracrystallinity was sometimes observed in bundles formed by rmC1, rm21, and rm17. The presence of low order diffraction peaks in a Fourier transform of an rm17-actin bundle (Fig. 5B) indicates gross regularity in filament packing. The reduction in bundling activity by rm14 and rmC1ΔC may arise from their lack of both exons II and VI, and they may be thought of as "double deletions" of the full-length 21.5 kDa transcript (Fig. 4A). The region derived from exon VI may be of particular importance, as it is part of a sequence comprising an amphipathic α-helix that may contribute to lipid- [30] and CaM-binding [31]. Although rm17 also lacks the region derived from exon VI, it does contain the exon II-derived sequence, a highly basic region with a linear charge density 60% greater than the average charge density of rm21.

Interaction of classic isoforms with calmodulin

The binding of Ca^{2+}-CaM to C1 or rmC1 is a complex event causing an increase in maximum intensity and a blue shift of the intrinsic Trp fluorescence [31], an effect abolished by the chelation of Ca^{2+}. The other classic isoforms described here were assayed under the same conditions, and all of them exhibited similar calcium-dependent CaM-binding properties (Supplementary Fig. 2). As for 18.5 kDa MBP [5,7], actin filaments polymerized by the other classic isoforms can be depolymer-

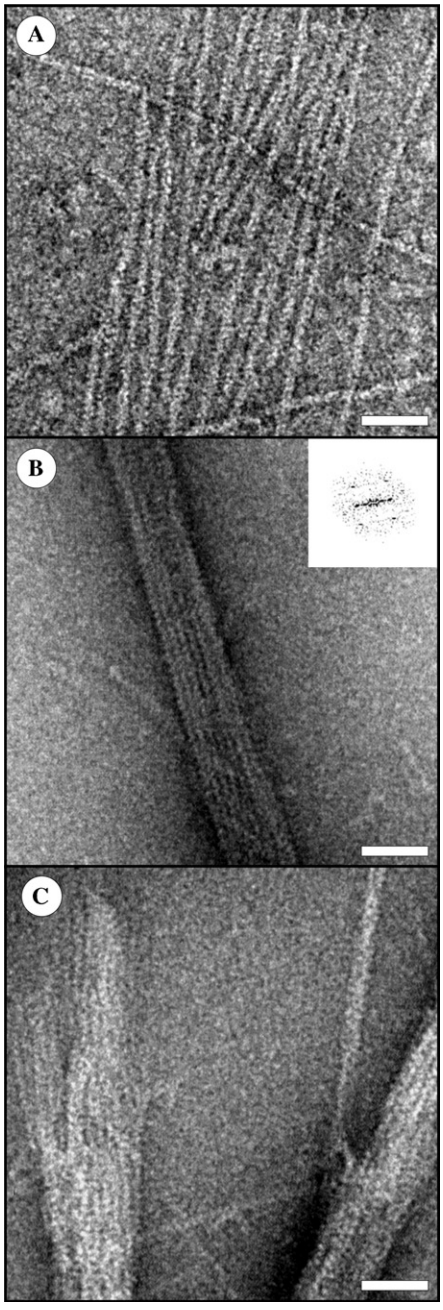

Fig. 5. Morphology of F-actin bundles formed by (A), rm14; (B), rm17; and (C), rm21. An equimolar amount of MBP was added to 2.5 μM actin pre-polymerized by 50 mM KCl and 2 mM $MgCl_2$, and incubated for 1 h prior to staining by 2% uranyl acetate. Scale bars represent 50 nm.

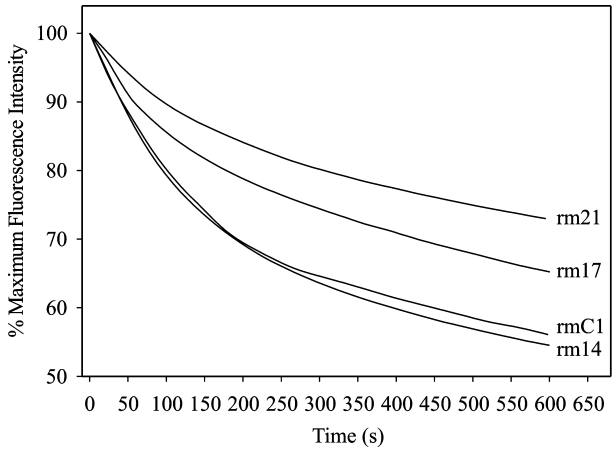

Fig. 6. Depolymerization of MBP–actin filaments induced by Ca^{2+}-calmodulin. Polymerization was effected by adding an isoform to 5 μM G-actin (5% pyrene labelled) in G-buffer at a 1:4 molar ratio. Depolymerization was initiated by adding Ca^{2+}-CaM at a molar ratio of 2:1 CaM/MBP.

ized by adding Ca^{2+}-CaM (Fig. 6). At a 2:1 molar excess of Ca^{2+}-CaM over MBP, the dissociation observed was slowest for rm21-actin filaments, fastest for rmC1-actin and rm14-actin filaments, and intermediate for rm17-actin filaments. The rate of depolymerization appeared to be a function of MBP charge. Although rmC1 and rm17 have the same net charge, rm17 is shorter and therefore has a higher charge density. This result is consistent with the observation that a recombinant mimic of deiminated MBP, of reduced cationicity, is more readily dissociated from F-actin by calmodulin than rmC1 [8].

Implications for MBP–actin interactions in oligodendrocytes

Our results demonstrate conclusively that alterations in the charge properties of MBP, i.e., electrostatics, can regulate its interaction with actin. The reduction in the extent of polymerization induced by modified charge isomers, both here and in a complementary study [8], is particularly intriguing, as their creation requires energy, and their roles in the oligodendrocyte are not understood [17]. The electrostatic nature of the MBP–actin interaction does not preclude a relevant physiological role [14,32], particularly in light of the cytoskeletal defects observed in *Shiverer* oligodendrocytes [12,13]. A reduction in actin-bundling activity may be important in the pathology of multiple sclerosis, where there is an increased amount of deiminated MBP [8]. Some species of MBP may represent effectors of process extension during myelinogenesis, an actin-mediated event, as suggested by a recent report that a Golli-MBP isoform is associated with actin and involved in the formation of dorsal ruffles, cleavage furrows, and processes [33].

Acknowledgments

The authors thank Drs. Anthony and Celia Campagnoni for expression constructs for recombinant 14, 17, and 21.5 kDa isoforms of murine MBP, Drs. Mario Moscarello and Denise Wood for charge isomers of 18.5 kDa bovine MBP, Dr. Joan Boggs for helpful comments, Ms. Lisa Hewer and Dr. F. Ross Hallett for assistance with preliminary light scattering assays, and Drs. Ian Tetlow and Michael Emes for the use of their FPLC system. This work was supported by the Natural Sciences and Engineering Research Council of Canada (G.H.), and by an Ontario Graduate Scholarship (C.M.D.H.).

Appendix A. Supplementary data

Supplementary data associated with this article can be found, in the online version, at doi:10.1016/j.bbrc.2005.01.151.

References

[1] N. Baumann, D. Pham-Dinh, Biology of oligodendrocyte and myelin in the mammalian central nervous system, Physiol. Rev. 81 (2001) 871–927.
[2] C. Richter-Landsberg, The oligodendroglia cytoskeleton in health and disease, J. Neurosci. Res. 59 (2000) 11–18.
[3] J. Song, B.D. Goetz, P.W. Baas, I.D. Duncan, Cytoskeletal reorganization during the formation of oligodendrocyte processes and branches, Mol. Cell. Neurosci. 17 (2001) 624–636.
[4] B. Barylko, Z. Dobrowolski, Ca^{2+}-calmodulin-dependent regulation of F-actin-myelin basic protein interaction, Eur. J. Cell Biol. 35 (1984) 327–335.
[5] Z. Dobrowolski, H. Osinska, M. Mossakowska, B. Barylko, Ca^{2+}-calmodulin-dependent polymerization of actin by myelin basic protein, Eur. J. Cell Biol. 42 (1986) 17–26.
[6] G.A. Roth, M.D. Gonzalez, C.G. Monferran, M.L. De Santis, F.A. Cumar, Myelin basic protein domains involved in the interaction with actin, Neurochem. Int. 23 (1993) 459–465.
[7] J.M. Boggs, G. Rangaraj, Interaction of lipid-bound myelin basic protein with actin filaments and calmodulin, Biochemistry 39 (2000) 7799–7806.
[8] J.M. Boggs, G. Rangaraj, C.M.D. Hill, I.R. Bates, Y.M. Heng, G. Harauz, Effect of arginine loss in myelin basic protein, as occurs in its deiminated charge isoform, on mediation of actin polymerization and actin binding to a lipid membrane in vitro, Biochemistry (2005) (in press), doi:10.1021/bi0473760.
[9] M.I. Givogri, E.R. Bongarzone, A.T. Campagnoni, New insights on the biology of myelin basic protein gene: the neural-immune connection, J. Neurosci. Res. 59 (2000) 153–159.
[10] G. Harauz, N. Ishiyama, C.M.D. Hill, I.R. Bates, D.S. Libich, C. Fares, Myelin basic protein-diverse conformational states of an intrinsically unstructured protein and its roles in myelin assembly and multiple sclerosis, Micron 35 (2004) 503–542.
[11] R.H. Woodruff, R.J. Franklin, The expression of myelin basic protein exon 1 and exon 2 containing transcripts during myelination of the neonatal rat spinal cord-an in situ hybridization study, J. Neurocytol. 27 (1998) 683–693.

[12] Y. Inoue, R. Nakamura, K. Mikoshiba, Y. Tsukada, Fine structure of the central myelin sheath in the myelin deficient mutant Shiverer mouse, with special reference to the pattern of myelin formation by oligodendroglia, Brain Res. 219 (1981) 85–94.
[13] C.A. Dyer, T.M. Philibotte, S. Billings-Gagliardi, M.K. Wolf, Cytoskeleton in myelin-basic-protein-deficient shiverer oligodendrocytes, Dev. Neurosci. 17 (1995) 53–62.
[14] J.X. Tang, P.A. Janmey, The polyelectrolyte nature of F-actin and the mechanism of actin bundle formation, J. Biol. Chem. 271 (1996) 8556–8563.
[15] A. Arbuzova, A.A. Schmitz, G. Vergères, Cross-talk unfolded: MARCKS proteins, Biochem. J. 362 (2002) 1–12.
[16] K.J. Amann, B.A. Renley, J.M. Ervasti, A cluster of basic repeats in the dystrophin rod domain binds F-actin through an electrostatic interaction, J. Biol. Chem. 273 (1998) 28419–28423.
[17] J.K. Kim, F.G. Mastronardi, D.D. Wood, D.M. Lubman, R. Zand, M.A. Moscarello, Multiple sclerosis: an important role for post-translational modifications of myelin basic protein in pathogenesis, Mol.Cell Proteomics 2 (2003) 453–462.
[18] D.D. Wood, J.M. Bilbao, P. O'Connors, M.A. Moscarello, Acute multiple sclerosis (Marburg type) is associated with developmentally immature myelin basic protein, Ann. Neurol. 40 (1996) 18–24.
[19] I.R. Bates, P. Matharu, N. Ishiyama, D. Rochon, D.D. Wood, E. Polverini, M.A. Moscarello, N.J. Viner, G. Harauz, Characterization of a recombinant murine 18.5-kDa myelin basic protein, Protein Expr. Purif. 20 (2000) 285–299.
[20] J.A. Cooper, S.B. Walker, T.D. Pollard, Pyrene actin: documentation of the validity of a sensitive assay for actin polymerization, J. Muscle Res. Cell Motil. 4 (1983) 253–262.
[21] E. Jo, J.M. Boggs, Aggregation of acidic lipid vesicles by myelin basic protein: dependence on potassium concentration, Biochemistry 34 (1995) 13705–13716.
[22] C.A. Dyer, The structure and function of myelin: from inert membrane to perfusion pump, Neurochem. Res. 27 (2002) 1279–1292.
[23] R. Zand, M.X. Li, X. Jin, D. Lubman, Determination of the sites of posttranslational modifications in the charge isomers of bovine myelin basic protein by capillary electrophoresis-mass spectroscopy, Biochemistry 37 (1998) 2441–2449.
[24] J.M. Boggs, P.M. Yip, G. Rangaraj, E. Jo, Effect of posttranslational modifications to myelin basic protein on its ability to aggregate acidic lipid vesicles, Biochemistry 36 (1997) 5065–5071.
[25] J.J. Ramwani, R.M. Epand, M.A. Moscarello, Secondary structure of charge isomers of myelin basic protein before and after phosphorylation, Biochemistry 28 (1989) 6538–6543.
[26] J.M. Boggs, G. Rangaraj, Effect of phosphorylation of myelin basic protein on its interaction with actin in vitro, J. Neurochem. 90 (2004) 73.
[27] C.M.D. Hill, J.D. Haines, C.E. Antler, I.R. Bates, D.S. Libich, G. Harauz, Terminal deletion mutants of myelin basic protein: new insights into self-association and phospholipid interactions, Micron 34 (2003) 25–37.
[28] J.B. Ulmer, P.E. Braun, In vivo phosphorylation of myelin basic proteins: single and double isotope incorporation in developmentally related myelin fractions, Dev. Biol. 117 (1986) 502–510.
[29] L. Pedraza, L. Fidler, S.M. Staugaitis, D.R. Colman, The active transport of myelin basic protein into the nucleus suggests a regulatory role in myelination, Neuron 18 (1997) 579–589.
[30] N. Ishiyama, I.R. Bates, C.M.D. Hill, D.D. Wood, P. Matharu, N.J. Viner, M.A. Moscarello, G. Harauz, The effects of deimination of myelin basic protein on structures formed by its interaction with phosphoinositide-containing lipid monolayers, J. Struct. Biol. 136 (2001) 30–45.
[31] D.S. Libich, C.M.D. Hill, I.R. Bates, F.R. Hallett, S. Armstrong, A. Siemiarczuk, G. Harauz, Interaction of the 18.5-kD isoform of myelin basic protein with Ca^{2+}-calmodulin: effects of deimination assessed by intrinsic Trp fluorescence spectroscopy, dynamic light scattering, and circular dichroism, Protein Sci. 12 (2003) 1507–1521.
[32] L.S. Jones, B. Yazzie, C.R. Middaugh, Polyanions and the proteome, Mol. Cell. Proteomics 3 (2004) 746–769.
[33] J.M. Feng, C.W. Campagnoni, Y.H. Hu, K. Kampf, V. Schonmann, A.T. Campagnoni, Golli product of myelin basic protein gene promotes process formation in neuronal cells. Neuroscience, 2004, Meeting of the Society for Neuroscience, San Diego, CA, 2004.